JOURNAL OF SPACECRAFT AND ROCKETS
Vol. 45, No. 4, July–August 2008

2009 Version of the Aeroprediction Code: AP09

F. G. Moore* and L. Y. Moore†
Aeroprediction, Inc., King George, Virginia 22485

DOI: 10.2514/1.35703

The 2005 version of the Aeroprediction Code (AP05) was evaluated when applied to configurations with boattails. Results of the evaluation indicated the AP05 predictions for normal force, center of pressure, and pitch and roll damping moments needed improvement. As a result, new and improved methods were developed and incorporated into the AP05 to be released as the AP09. Improvements include body-alone lift characteristics for Mach numbers less than two, low angle-of-attack improvements for roll and pitch damping for configurations with long boattails, incorporation of an improved boundary-layer displacement model, and refinement of several other existing methods. In addition, new methods were developed to predict nonlinear roll and pitch damping. Comparing the new and improved methods to existing experimental data indicated significant improvements in roll and pitch damping, normal force, and center of pressure predictions compared to the AP05. However, validation of the AP09 code was not as complete as desired due to limited generic nonlinear roll and pitch damping data. Also, most of the available nonlinear dynamic derivative data have larger than desired accuracy boundaries due to model sting and wind-tunnel wall interference issues. The AP09 also calculates static margin based on tangent (derivative of normal force at a given angle of attack) as well as secant slope (value of normal force over sine of the angle of attack) values of normal force and pitching moment coefficients. Weapons affected most by the new AP09 methodology are mortars, low-drag bombs, and projectiles, in that order. However, the nonlinear dynamic derivative predictions affect all weapons. The AP09 is thus the most accurate and robust of the Aeroprediction Codes to date.

Nomenclature

A_{REF}	=	reference area (maximum cross-sectional area of body, if a body is present, or planform area of wing, if wing alone), ft^2
b	=	wingspan (not including body), ft
C_A	=	axial force coefficient
C_{ℓ_p}	=	roll damping moment coefficient, $\gamma C_\ell/\gamma(pd/2V_\infty)$
C_M	=	pitching moment coefficient (based on reference area and body diameter, if body present, or mean aerodynamic chord, if wing alone)
$C_{M_q} + C_{M_{\dot\alpha}}$	=	pitch damping moment coefficient, $\lfloor C_M(q)/(qd/2V_\infty) + C_M(\dot\alpha)/(\dot\alpha d/2V_\infty)\rfloor$
C_{M_α}	=	pitching moment coefficient derivative. per radian
C_N	=	normal force coefficient
C_{N_α}	=	normal force coefficient derivative, per radian, due to angle of attack or control deflection, respectively
c, c_r, c_t	=	local chord, root, and tip chord, respectively, ft
d_B	=	body base diameter, ft
d_N	=	diameter of truncated nose tip, ft
d_{ref}	=	reference body diameter, ft
ℓ, ℓ_n, ℓ_a, ℓ_B	=	total body, nose, afterbody, or boattail length, respectively, ft or cal
M_∞	=	freestream Mach number
p, q	=	roll and pitch rate, respectively, rad/s
$X_{\text{c.g.}}$	=	distance to center of gravity, ft
$X_{\text{c.p.}}/d$	=	center of pressure (calibers from some reference point)
x, y, z	=	coordinate system, x along body axis, y out right wing, z up
α	=	angle of attack, deg
δ	=	control deflection, deg
θ_b	=	boattail angle, deg
Φ	=	roll position of missile fins; $\Phi = 0$ deg corresponds to fins in the plus (+) orientation; $\Phi = 45$ deg corresponds to fins rolled to the cross (×) orientation

Received 15 November 2007; revision received 29 February 2008; accepted for publication 29 February 2008.

*President; drfgmoore@hotmail.com. Associate Fellow AIAA.
†Computer Scientist.

Introduction

THIS paper documents the new theoretical elements that have been integrated into the 2005 version (AP05) of the Aeroprediction Code (APC) to form the 2009 version of the APC, the AP09. The AP09 is the 10th version of the APC developed. The first three versions of the APC (AP72, AP74, and AP77) were aimed at meeting unguided and guided projectile requirements. The next four versions of the APC (AP81, AP93, AP95, and AP98) addressed missile requirements, which tend to fly at higher Mach numbers and angles of attack (AOA), and also to have more general body geometries then projectiles. AP02 met many projectile needs that had emerged over about a 25-year period between 1977 and 2002. AP05 addressed several additional projectile and weapon needs, along with continuing to improve productivity and making the APC more robust. The AP09 addresses improved accuracy of both static and dynamic aerodynamics for configurations with boattails and for the first time develops new methodology to allow nonlinear values of pitch and roll damping to be computed. Moore [1] documents the theory of the first seven versions of the APC, [2] documents the AP02 theory, and [3] documents the AP05 theory. Table 1 summarizes the evolution of the APC from its inception in 1972 to the AP09.

A few years ago, Aeroprediction, Inc. (API) was providing aerodynamic support to the Naval Surface Warfare Center, Dahlgren Division (NSWCDD) on a mortar round. API calculated normal force, axial force, pitching moment, center of pressure, and roll and pitch damping moments for a wide variety of Mach numbers and angles of attack for several different mortar configurations. After the aerodynamic computations were complete, a set of experimental data on one of the configurations was made available to API. In comparing the AP05 predictions to experimental data, it was obvious that a large boundary layer was present on the long boattail of the mortar, negating some of the fin effectiveness in providing static stability, along with reducing roll and pitch damping.

Table 1 Evolution of Aeroprediction Code in terms of new added capability

			Flight conditions								
Version	Weapon	Aerodynamics	Mach no.	Read gas avail.	AOA range, deg	Roll, deg	Trajectory avail.	Nonlinear distributed loads avail.	Computers	Emerging projectile needs	Nonlinear dynamic derivatives
1972	Axisymmetric unguided projectiles	Static only	0–3	No	0–15	$\Phi = 0$	No	No	CDC	No	No
1974	Axisymmetric unguided projectiles, rockets, missiles	Same	0–3	No	0–15	$\Phi = 0$	No	No	CDC	No	No
1977	Same	Static and dynamic	0–3	No	0–15	$\Phi = 0$	No	No	CDC, IBM	No	No
1981	Same	Same	0–8	No	0–15 (limited conf. at higher α)	$\Phi = 0$	No	No	CDC, IBM, VAX	No	No
1993	Same	Same	0–20	Yes	0–30	$\Phi = 0$	No	No	CDC, IBM, VAX, Silicon Graphics	No	No
1995	Same	Same	0–20	Yes	0–90	$\Phi = 0$	No	No	Interactive PC	No	No
1998	Axisymmetric and asymmetric missiles, rockets	Same	0–20	Yes	Same	$\Phi = 0$, 45	No	Yes	Interactive PC, Windows 98 only	No	No
2002	Same + 6, 8 fin	Same	0–20	Yes	Same	Same	Yes	Yes	Improved interactive PC, Windows 98, 2000 and NT	Yes	No
2005	Same + 3 fin	Same + trim aero output	0–20	Yes	Same	Same	Yes with alt. inc.	Yes	Same + XP	Yes + addt′l req. met	No
2009	Same	Imp. for boattails	0–20	Yes	Same	Same	Same	Yes	Same	Same	Yes

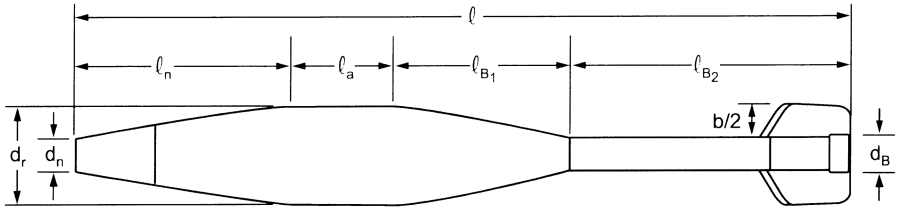

a) Typical mortar configuration

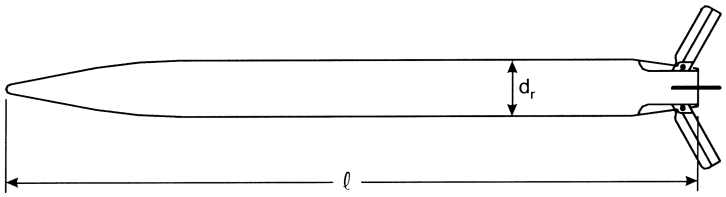

b) Schematic of guided projectile

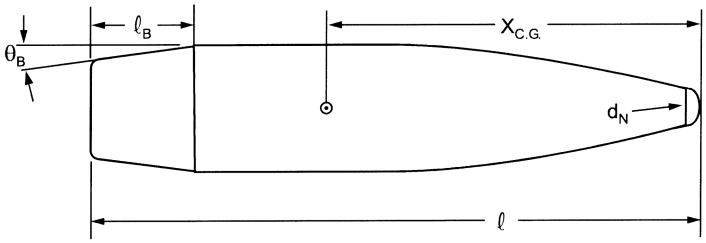

c) Spin-Stabilized projectile

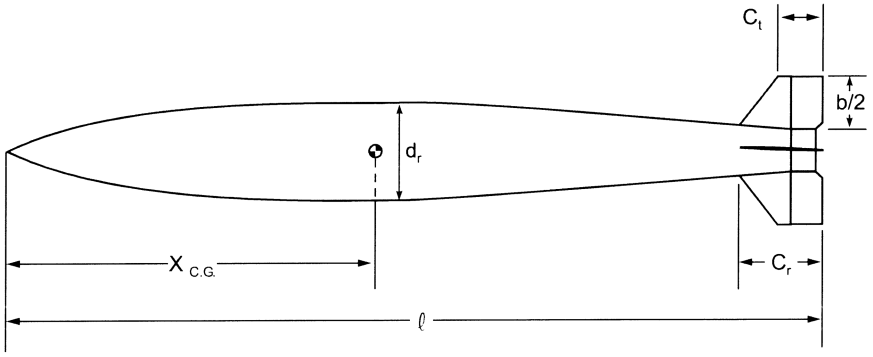

d) Low-Drag bomb

Fig. 1 Some typical weapons with boattails.

During the last 3 years, API undertook an evaluation of the weak areas of the AP05 when used on weapons with boattails, as well as developing new or improved ways to address the weak areas. This paper serves to summarize the weak areas of the AP05 and methods developed to overcome or improve upon the weak areas. However, only a summary of the theory will be given, as previous documentation ([4–7]) has the detailed theoretical derivations and more examples included as well. Finally, several examples are given to show the improvement of the AP09 over the AP05 for configurations with and without boattails. The weapons affected (see Fig. 1) are primarily mortars, low-drag bombs, spin-stabilized projectiles, and some missiles.

In addition to boattailed configuration aerodynamic prediction weaknesses, the AP05 and all prior versions of the Aeroprediction Code have only linear values of roll and pitch damping. Many weapons can oscillate or rotate at AOA, due to launch conditions or low static margin which can cause the dynamic derivatives to become nonlinear. The nonlinear dynamic derivatives can have significant effects on the flight performance of unguided weapons and, to a lesser extent, guided weapons. No generic wind-tunnel database is available to allow accurate estimation of pitch and roll damping nonlinearities. However, there are limited dynamic derivative databases available for specific configurations. As a result, the AP09 will provide a nonlinear prediction capability for roll and pitch damping. Unfortunately, because there is no "truth" model to validate the nonlinear dynamic stability predictions, refinements to the new methods at a later time are probable. On the other hand, the AP09 will be the first semi-empirical code to provide nonlinear predictions of roll and pitch damping moments.

Summary of New Methods for AP09

The AP09 theory will be briefly summarized in two parts: the theory of the AP72 up through the AP05, and then the new and improved methods added to the AP05 which make up the AP09. As already mentioned, the theory of the first nine versions of the APC is discussed in [1–3]. In general, all versions of the APC are based on slender body theory, linear theory, and second-order theory at low AOA, and empirical methods at high AOA. The low-AOA theoretical methods give the APC a good foundation to predict aerodynamics for various geometries and for various flight conditions up to an AOA of about 10 deg. The empirical methods

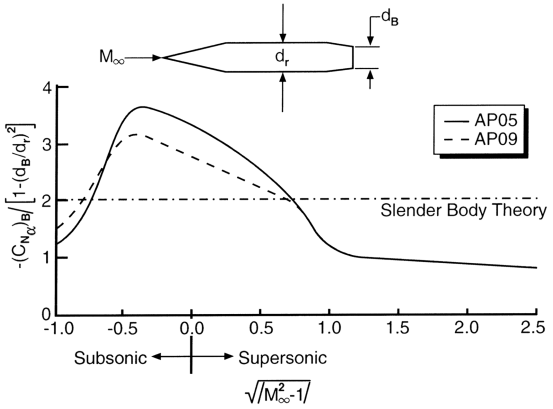

Fig. 2 Decrease in C_{N_α} due to boattail.

were developed based on large wind-tunnel component databases, in conjunction with total configuration databases, and allowed the low-AOA theoretical methods to be extended to 90 deg AOA. The overall approach of combining the low-AOA methods with the wind-tunnel databases to form a semi-empirical APC is described in [1], Chaps. 3 and 5. It is emphasized here that the key to the accuracy of the APC at low AOA is the emphasis on theoretical methods, and the key to the accuracy at high AOA is the use of large generic wind-tunnel databases to develop approximations to aerodynamics based on various geometry and Mach number variations. The combination of low-AOA theory and high-AOA databases is what makes the APC a semi-empirical code vs an empirical code where empirical methods are used at all angles of attack and an all theoretical code where no empirical methods are used.

Three areas were addressed in the AP09 for improvements in accuracy or to add additional capability to the code. The accuracy improvements primarily dealt with configurations with boattails at low AOA. Generally speaking, the longer the boattail, the greater the accuracy improvements. The other two areas addressed were to develop new capability to allow nonlinear values of both pitch and roll damping to be predicted. Each of the three areas will be summarized in the discussion that follows.

Low-AOA Improvements for Configurations with Boattails

The API review of the AP05, as applied to configurations with boattails, was very thorough and, unfortunately, found several areas where improvements were needed. Each area where improvements were made for the AP09 will be briefly summarized. Again for details of the theory, the reader is referred to [4,7]. The first area where improvements were made was body-alone lift characteristics. For Mach numbers less than 1.2, the body-alone lift characteristics for the nose were changed from empirical in the AP05 to slender body theory in the AP09. For the afterbody term, little change was made. On the other hand, the boattail normal force term was changed more noticeably for Mach numbers less than 1.2, as seen in Fig. 2. Note that in Fig. 2, the boattail negative normal force term is reduced somewhat for the AP09 compared with the AP05. For Mach numbers greater than 1.2, where the hybrid theory of Van Dyke (HTVD) is used for the normal force and center of pressure predictions, it was found that the HTVD consistently gave values of boattail normal force that were too high in magnitude for the low supersonic Mach number range $1.2 \leq M_\infty < 2.0$. The boattail term was reduced by an empirical factor to be in closer agreement with experimental data.

A second improvement for low AOA was for body-alone pitch damping for cases in which the boattail is greater than about a caliber in length. The AP05 gave values of body-alone pitch damping that were much too high. Again, an empirical factor was derived, using experimental data, to modify the AP05 body-alone pitch damping as a function of Mach number and body base diameter.

If the configuration has fins located on the boattail, several more improvements were made. These improvements included refinements for the multifin factors used in the Aeroprediction Code for calculating lifting characteristics of noncruciform configurations, modifications to the effective radius of the body for roll and pitch damping, elimination of the double counting of the body length underneath the wings in roll and pitch damping, accounting for the boundary-layer displacement effect on fins, and refinement of the nonlinear axial force for body–tail cases. Again, detailed discussion of these problem areas and theoretical modifications made for the AP09 are given in [4,7].

Nonlinear Pitch Damping

The AP05 and all prior versions of the APC contain only linear values of pitch and roll damping moments. Two new nonlinear methods were developed for pitch damping moments [5,7] and a new method was also developed for estimating nonlinear roll damping moments [6,7]. The new nonlinear dynamic derivative methods developed were limited by a scarcity of data, as well as by accuracy concerns of much of the pitch damping data. As a result, it is likely that the new nonlinear methods will be refined if more nonlinear pitch and roll damping data become available.

The two new methods developed to predict nonlinear pitch damping are both included in the AP09 tabular listing. These methods, referred to here as methods 2 and 3, each have advantages and disadvantages. Method 2 uses the structural load methodology in the AP05 for Mach numbers greater than 1.2 and extends this methodology to Mach number zero. Method 2 then takes each local load on the body and computes a local pitch damping term, and sums the local body terms to get the total pitch damping. Initially, the fins were treated as a point for pitch damping calculations. However, it was found that greater accuracy could be obtained for fins (particularly those with longer chords) by using the structural loads on the fins to compute local pitch damping for various chordwise segments. These local fin pitch damping values were then summed to obtain the fin pitch damping. Of course, all the nonlinear static aerodynamics of the APC were used in the computation of the nonlinear pitch damping for method 2. Method 2 is very robust in the sense that it will handle all angles of attack (0–90 deg), Mach numbers (0–20), roll orientations (0, 45 deg), control deflections, and

Table 2 Summary of method 2 and 3 approaches to predict nonlinear pitch damping moments

Method 2: use static aerodynamics completely
1) Uses all nonlinear static aerodynamics of AP09 and structural loads to distribute body loads
2) Very robust in α, M_∞, δ, Φ, number of fins
3) Distributes fin loads over 100 equally spaced chordwise locations
4) Predicts local body pitch damping
5) Has minimum empiricism
6) More difficult to implement than method 3
Method 3: uses quasi-time-dependent wing-alone solution and combines with improved empirical body-alone pitch damping
1) Uses all improved body-alone pitch damping of AP09 for $\alpha = 0$ deg
2) Uses quasi-time-dependent wing-alone solution
3) Uses a simple method to relate zero α aero to AOA
4) More empirical and somewhat less robust (no Φ dependence) than method 2

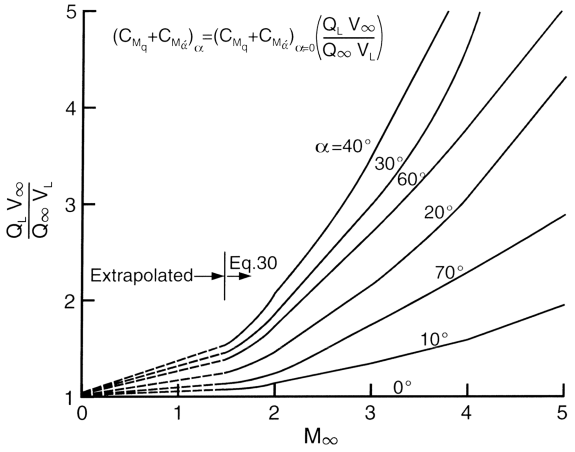

Fig. 3 Approximate relationship to allow pitch damping nonlinearities to be estimated based on $C_{M_q} + C_{M_{\dot\alpha}}$ at AOA zero.

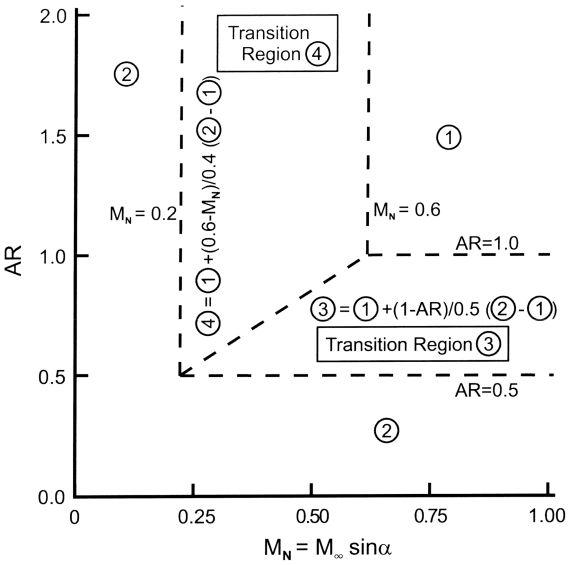

Fig. 4 Area of applicability of methods 1 and 2 to predict roll damping as function of aspect ratio and normal Mach number.

multifin options that the AP09 code allows. Method 2 also calculates local body pitch damping moments and has much less empiricism than method 3 does. On the other hand, it was much more involved and difficult to implement than method 3, even though the AP09 code already had all the nonlinear static aerodynamics and structures loads available for $M_\infty \geq 1.2$.

Method 3 uses the original time-dependent linear solution for $C_{M_{\dot\alpha}}$ and rotational pitching rate C_{M_q} from linear theory. Method 3 uses the improvements in pitch damping due to long boattails derived for the AP09. Method 3 was based on derivation of a term, using Newtonian theory, to multiply the improved low-AOA pitch damping values to obtain nonlinear values at AOA. Equation (1) is the final formula derived for multiplying low-AOA pitch damping to obtain high-AOA pitch damping. Method 3 was also much easier to implement than method 2. Table 2 summarizes the method 2 and method 3 approaches.

$$\frac{Q_L V_\infty}{Q_\infty V_L} = \cos\alpha\left[\frac{1+[(\gamma-1)/2]M_\infty^2\cos^2\alpha}{1+[(\gamma-1)/2]M_\infty^2}\right][1+\gamma M_\infty^2\sin^2\alpha] \quad (1)$$

Figure 3 shows how Eq. (1) varies with AOA. Figure 3 also indicates a lower Mach number boundary for applying Eq. (1) as 1.5. Below Mach 1.5, linear extrapolation to a value of 1.0 at Mach number zero is assumed for Eq. (1).

Nonlinear Roll Damping

Two different approaches were examined to predict nonlinear roll damping moments. Here nonlinear refers to nonlinearities in AOA, not roll rate. One method considered the physical phenomena of compressibility and viscous effects as the primary driver. The other approach considered wing aspect ratio and stall effects as the primary drivers. Fortunately, these two approaches were best in certain areas of aspect ratio and normal Mach number, and so the two approaches could be integrated together in a single overall method. It was found that for low normal Mach numbers ($M_N = M_\infty \sin\alpha$) or low wing aspect ratio, the approach that focuses in on the physical phenomena of wing aspect ratio and stall effects worked best (method 2 of Fig. 4). For cases where the normal Mach number was fairly high or the aspect ratio was fairly high, the method that focused on the physical phenomena of compressibility and viscous effects worked best (method 1 of Fig. 4). There was a transition region (see Fig. 4) where the two methods were blended together as a function of normal Mach number and wing aspect ratio. The reader is referred to [6,7] for more details of the new roll damping method.

Finally, the AP05 and all prior versions of the APC use the secant $[C_{N_\alpha} = C_N/\sin(\alpha)]$ vs the tangent slope $(C_{N_\alpha} = \mathrm{d}C_N/\mathrm{d}\alpha)$ to compute normal force and pitching moment coefficient derivatives as well as center of pressure. The AP09 will use the correct tangent slope value for C_{N_α}, C_{M_α}, and $X_{\text{c.p.}}$ as opposed to the secant slope. However, for reference purposes to the AP05 outputs, the center of pressure computed by the secant slope will also be included in the AP09 tabular listing. Table 3 summarizes the new and improved methods included in the AP09.

Results and Discussion

A summary of the results of the new methods discussed in the section Summary of Theory, as applied to configurations similar to those in Fig. 1, will be given. More detailed results can be found in [4–7]. Many of the configurations that aerodynamic comparisons have made are limited distribution (i.e., U.S. Government agencies and their contractors). For limited distribution cases, only error comparisons of the AP09 compared with data can be given. These error comparisons are defined for each aerodynamic coefficient as follows:

Table 3 AP09 new or improved methods

AP09 improved methods
1) Body-alone lift characteristics for $M_\infty < 1.2$
2) Body-alone lift characteristics for $M_\infty \geq 1.2$
3) Body-alone pitch damping characteristics for configurations with long boattails
4) Multifin factors for low aspect ratio wings at subsonic speeds
5) Linear roll and pitch damping improvements for finned configurations with long boattails
6) Incorporation of boundary-layer displacement effects on body–tail configurations with long boattails
7) Nonlinear axial force modifications for body–tail configurations
8) Tangent slope for C_{N_α} and C_{M_α}
AP09 new methods
1) Two methods for nonlinear pitch damping
2) Nonlinear roll damping

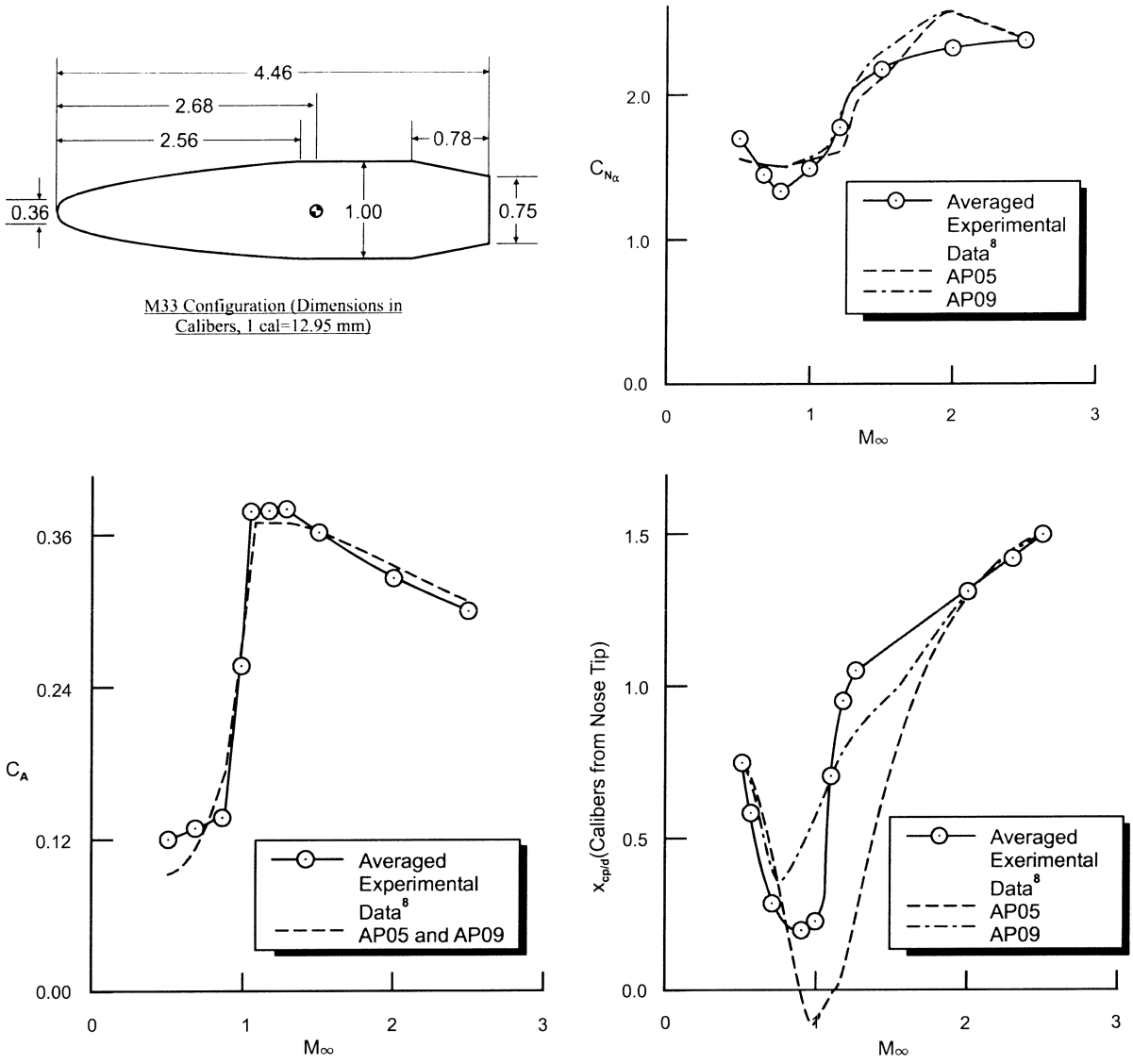

Fig. 5 Comparison of AP05 and AP09 aerodynamic predictions to experimental data for M33 projectile.

$$\text{percent error} = \frac{|C_{\text{exp}} - C_{\text{theory}}|}{C_{\text{exp}}} \times 100 \tag{2}$$

For center of pressure, the errors will be defined in terms of percent of body length. That is,

$$\frac{[(X_{\text{c.p.}})/d]_{\text{error}}}{\ell} = \frac{|[(X_{\text{c.p.}})_{\text{exp}}/d] - [(X_{\text{c.p.}})_{\text{theory}}/d]|}{\ell} \times 100 \tag{3}$$

In addition to error comparisons of the AP05 and AP09 compared with experimental data, improvements in error of the AP09 over the AP05 for various aerodynamic coefficients can be defined as

$$\text{AP 09 improvement in aerodynamics over the AP05} = \frac{\text{AP05 avg error (in percent)} - \text{AP09 avg error (in percent)}}{\text{AP05 avg error in percent}} \tag{4}$$

Equation (4) can be used for each of the aerodynamic coefficients that were computed by each code. For unlimited distribution cases, configurations, aerodynamics, and error comparisons can be shown.

The first set of data is for spin-stabilized unguided projectiles. Four configurations are considered, with only the M33 [8] being unlimited distribution. Figure 5 compares the AP09 static aerodynamic predictions to the AP05 and experimental data for the M33 at

Table 4 Comparison of average static aerodynamic prediction errors of AP05 and AP09 compared with experimental data for four boattailed projectiles

Configuration	C_A errors, %		AP09 improv. over AP05, %	C_{N_α} errors, %		AP09 improv. over AP05, %	$X_{\text{c.p.}}/d$ errors, % of body length		AP09 improv. over AP05, %
	AP05	AP09		AP05	AP09		AP05	AP09	
1) 155 mm [9]	6.9	6.9	0.0	4.6	3.4	26.1	6.1	5.2	14.8
2) M33 [8]	5.1	5.1	0.0	5.5	5.5	0.0	5.4	3.5	35.2
3) 5″/54 MK41 [10]	7.9	7.9	0.0	7.2	4.2	41.7	9.8	6.5	33.7
4) Hi frag [11]	5.0	5.0	0.0	12.6	3.9	67.4	8.2	1.2	85.4
Average	6.2	6.2	0.0	7.5	4.3	42.7	7.4	4.1	44.6

Table 5 Comparison of average static and dynamic aerodynamic prediction errors of AP05 and AP09 compared with experiment for several mortar rounds

Static aerodynamics									
Configuration	C_A errors, %		AP09 improv. over AP05, %	C_N errors, %		AP09 improv. over AP05, %	$X_{c.p.}/d$ errors, % of body length		AP09 improv. over AP05, %
	AP05	AP09		AP05	AP09		AP05	AP09	
1) 81 mm mortar [12]	10.1	9.5	5.9	33.3	13.7	58.9	2.6	1.4	46.0
2) XM 984 (194441) [13]	15.1	11.8	21.9	24.5	13.2	46.1	5.3	6.3	−18.2
3) XM 984 (194541) [13]	14.4	11.5	20.1	12.4	5.1	58.9	6.8	5.8	14.7
4) PGMM (11111) [14]	12.2	17.5	−43.4	27.8	14.1	49.3	7.6	2.1	72.3
5) PGMM (51511) [15]	13.1	19.6	−49.6	30.1	14.7	51.2	6.8	2.4	64.7
6) M49A4 [16]	21.6	12.7	41.2	35.6	11.1	38.8	77.0	6.7	91.3
Average	14.4	13.8	4.2	27.3	12.0	56.0	17.7	4.1	76.8

Dynamic derivatives						
Configuration	C_{ℓ_p} errors, %		AP09 improv. over AP05, %	C_{M_q} errors, %		AP09 improv. over AP05, %
	AP05	AP09		AP05	AP09	
1) 81 mm mortar [17]	40.1	13.0	67.6	232.4	7.4	96.8
2) PGMM (11111) [14]	104.5	35.5	66.0	288.3	13.3	95.3
3) PGMM (51511) [15]	102.3	33.7	61.1	204.8	8.5	95.8
Average	82.3	27.4	66.7	241.8	9.7	96.0

approximately 2 deg AOA. For this configuration, the only coefficient where the AP09 shows significant improvement over AP05 predictions is the center of pressure.

Table 4 now averages the errors for four projectile configurations for both the AP05 and AP09 compared with data. The errors are determined near zero AOA and at increments in Mach number of 0.1, from Mach number 0.5–2.5 using averaged experimental data. As seen in the table, the overall axial force coefficient error for both the AP05 and AP09 is 6.2%. The normal force coefficient slope error of the AP09 is 4.3% compared with 7.5% for the AP05, or a 42.7% reduction. The largest error reduction was for the Hi Frag projectile which had the largest boattail. The average center of pressure error for the AP09 was 4.1%, close to the goal of ±4%, whereas the AP05 center of pressure error was 7.4%, well above the ±4% goal. The AP09 thus decreased the average center of pressure error of the AP05 by 44.6%. It should be pointed out that Table 4 averages out C_A, C_N, and $X_{c.p.}$ errors over a range of Mach numbers for four different configurations. Detailed comparisons vs Mach number for each configuration is given in [4], which also shows, in general, the best accuracy at supersonic speeds (generally less than 5% error) and the worst accuracy at transonic Mach numbers (where worst case errors are 10–40%).

In summary, the improvements in body-alone normal force and center of pressure prediction for projectile configurations with boattails has provided substantial improvement in the AP09 prediction accuracy for these coefficients compared with the AP05. The largest error improvements occurred for the longest boattail case. No changes in axial force prediction errors were seen between the AP05 and AP09 for spin-stabilized projectiles.

All mortar configurations were limited distribution, and so only error comparisons of the AP09 to the AP05 and experimental data can be given. The error comparisons for the static aerodynamics include both AOA and Mach number with at least 12 data points (one data point is one Mach number and one AOA) included in the average for each configuration. For dynamic derivative error comparisons, only variations in Mach number are considered in the averages for each configuration. Nonlinearities in dynamic derivatives will be considered later.

Table 5 gives a summary of the static and dynamic aerodynamic prediction errors of the AP05 and AP09 for mortar configurations. Note that there are six configurations for static aerodynamics and only three for dynamic derivatives. As seen in the summary table, the axial force coefficient for the AP09 is only slightly superior to the AP05, with the AP09 being superior on four cases and inferior to the AP05 on the other two configurations. The AP09 normal force and center of pressure prediction on average are much better than the AP05. The AP05 normal force prediction error is cut in half by the AP09 (12.0 vs 27.3%) and the center of pressure error is reduced by

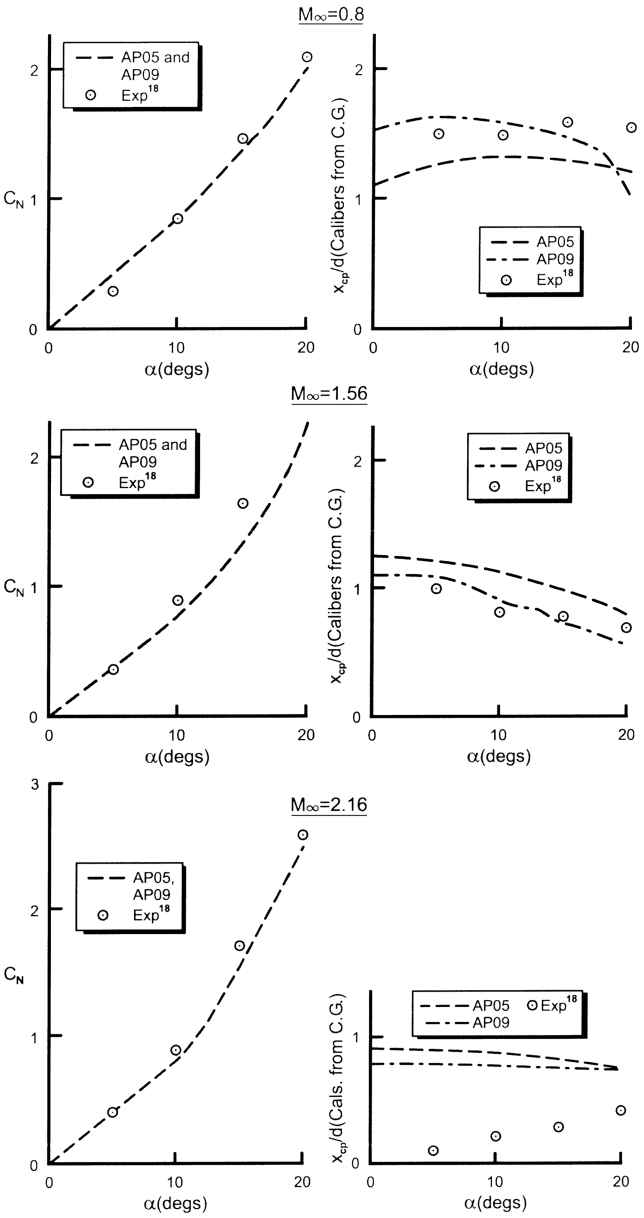

Fig. 6 Normal force and center of pressure comparisons of AP05 and AP09 to experiment ($\Phi = 0$ deg) for GPLDB.

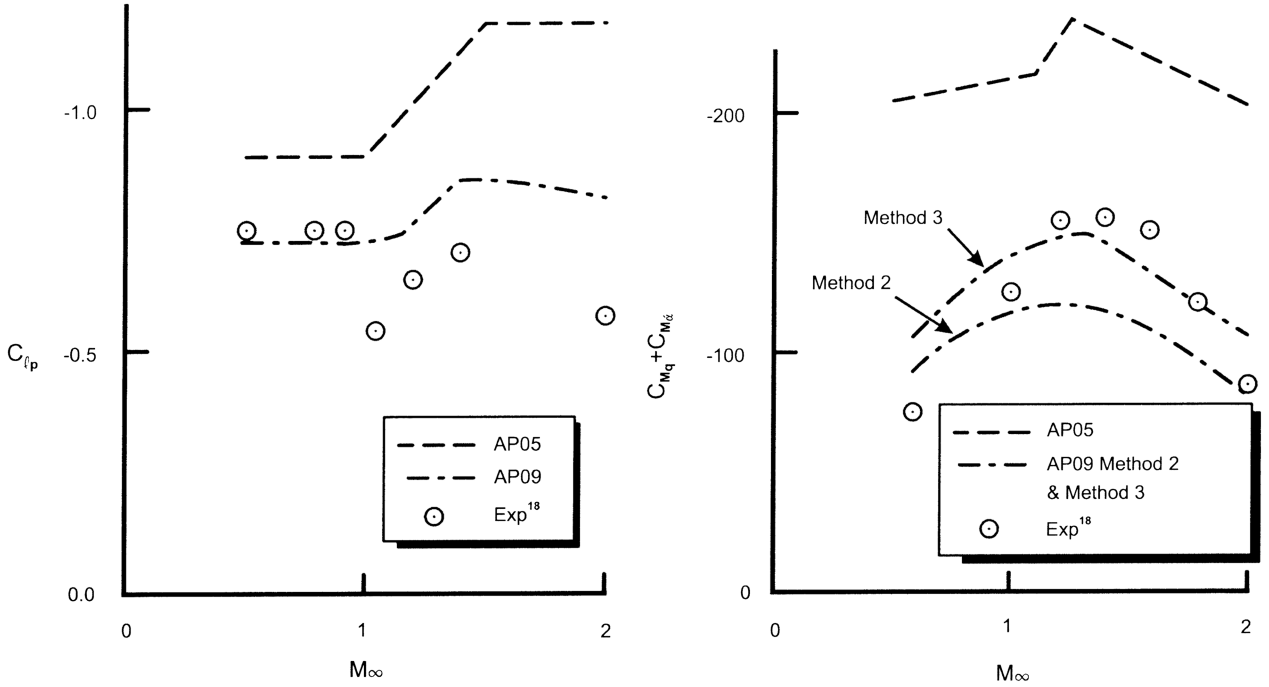

Fig. 7 Roll and pitch damping comparisons of AP05 and AP09 to experiment for GPLDB ($\Phi = 0$ deg).

over 75% (4.1 vs 17.7% of body length). The area of largest improvement of the AP09 over the AP05 is dynamic derivatives. The C_{ℓ_p} errors are reduced from 82.3 to 27.4% and the C_{M_q} errors are reduced from 241.8 to 9.7% when using the AP09 compared with the AP05. It is therefore clear that the AP09 shows substantial improvement over the AP05 on all mortar aerodynamics except for axial force, where the AP09 shows only a small improvement in accuracy over the AP05.

Several of the low-drag bomb concepts were unlimited distribution, and so aerodynamic results can be shown. The configuration considered here is the general purpose low-drag bomb (GPLDB) of Fig. 1d. Figure 6 shows a comparison of the AP05 and AP09 C_N and $X_{\text{c.p.}}$ to experiment [18] at Mach numbers of 0.8, 1.56, and 2.16 and AOA 0–20 deg. Note the AP05 and AP09 normal force coefficients are nearly identical but the AP09 gives improved center of pressure prediction over the AP05 at all three Mach numbers considered. Figure 7 shows comparisons of pitch and roll damping between experiment and the AP05 and AP09 predictions for small angle of attack as a function of Mach number. Note the significant improvement in dynamic derivative predictions of the AP09 over the AP05 and, in particular, the pitch damping predictions.

Table 6 now summarizes all the errors for five bomb configurations. Only two cases have axial force data, and so the accuracy averages here are not as reliable due to a smaller sample. Also, only four of the five configurations had roll and pitch damping data available. Several points are worth making in viewing Table 6. First, the AP09 improves aerodynamic estimates of all static and dynamic predictions compared with the AP05. Errors of the AP09 are reduced by 22.4% for axial force, 20% for normal force, 7.1% for center of pressure, 80.1% for roll damping, and 66.8% for pitch damping when compared with the AP05. Second, both the AP05 and AP09 give average errors within the ±10% desired range for C_N and ±4% ℓ_B for $X_{\text{c.p.}}/d$. Third, the AP09 provides significant improvement in pitch and roll damping compared with the AP05.

Figures 5–7 and Tables 4–6 primarily focus on the modifications added to the AP09 to improve the aerodynamic estimates of weapons

Table 6 Comparison of average static and dynamic aerodynamic prediction errors of the AP05 and AP09 compared with experiment for several bomb configurations.

Bomb static aerodynamic summary

Configuration	C_A errors, %		AP09 improv. over AP05, %	C_N errors, %		AP09 improv. over AP05, %	$X_{\text{c.p.}}/d$ errors, % of body length		AP09 improv. over AP05, %
	AP05	AP09		AP05	AP09		AP05	AP09	
1) MK82 GPLDB [18]	17.3	10.7	38.2	5.5	4.5	18.2	2.6	2.4	7.7
2) MK82 FF [19,20]	——	——	——	4.8	2.6	45.8	3.8	2.2	42.1
3) MK82 ISR [19,20]	——	——	——	10.0	11.4	−14.0	1.7	2.1	−23.5
4) MK82 ISRE [19,20]	——	——	——	8.5	7.1	16.5	1.9	3.5	−84.2
5) M117 [21,22]	12.0	12.0	0.0	4.0	4.0	0.0	3.8	2.8	26.3
				8.9	3.7	61.2			
Average	14.7	11.4	22.4	7.0	5.6	20.0	2.8	2.6	7.1

Bomb dynamic aerodynamics summary

Configuration	C_{ℓ_p} errors, %		AP09 improv. over AP05, %	C_{M_q} errors, %		AP09 improv. over AP05, %
	AP05	AP09		AP05	AP09	
1) MK82 GPLDB [18]	35.8	9.9	72.3	109.9	24.5	77.7
2) MK82 FF [19,20]	21.3	8.3	61.0	36.6	16.2	55.7
3) MK82 ISR [19,20]	26.4	0.2	99.2	8.4	8.0	4.8
4) MK82 ISRE [19,20]	28.8	4.0	86.1	17.6	8.3	52.8
Average	28.1	5.6	80.1	43.1	14.3	66.8

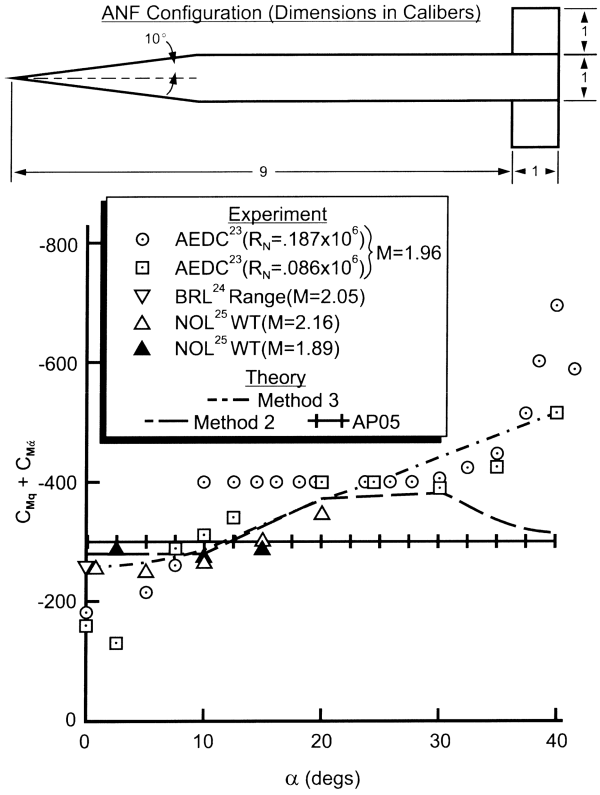

Fig. 8 Comparison of theory and experiment for pitch damping of ANF ($M_\infty \approx 2.0$).

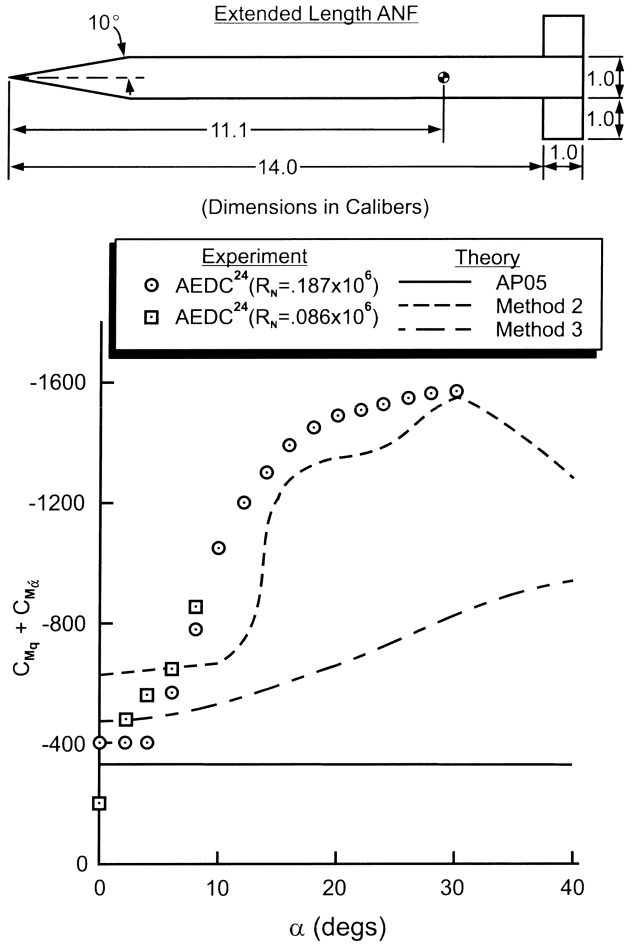

Fig. 9 Comparison of theory and experiment for pitch damping for extended length ANF ($M = 1.96$).

with boattails when flying at small angle of attack. The next series of figures will illustrate the new nonlinear dynamic derivatives methodology added to the APC. The first two examples are the pitch damping results at about $M_\infty = 2$ for the Army Navy finner (ANF) and an extended length ANF shown in Figs. 8 and 9, respectively. Figure 8 illustrates the fact that method 2 compares better to one data set, whereas method 3 compares better than method 2 to the Arnold Engineering Development Center (AEDC) data. Of course, all AP05 predictions of roll and pitch damping are independent of AOA.

Figure 9 is an extended length (15 vs 10 cal) ANF. Experimental data is taken from [24] at $M_\infty = 1.96$. By extending the length of the ANF by 5 cal, it is seen that the pitch damping increases greatly with AOA due to the large body term. It is also seen that method 2, which included all the nonlinear body loads from the AP09, is clearly superior to method 3 and the AP05.

The third configuration considered for pitch damping is the MK 82 low-drag bomb with data taken from [18]. Results are shown in Fig. 10 for $M_\infty = 2.16$, 1.56, and 0.8 to AOA 40 deg. Here, methods 2 and 3 are far superior to the AP05, due in part to the large boattail. Also, method 2 is slightly better than method 3 at $M_\infty = 2.16$ and 0.8, and method 3 is slightly better than method 2 at $M_\infty = 1.56$.

Figures 11–15 compare the new nonlinear roll damping method to the linear AP05 theory and experimental data. Figure 11 is the ANF

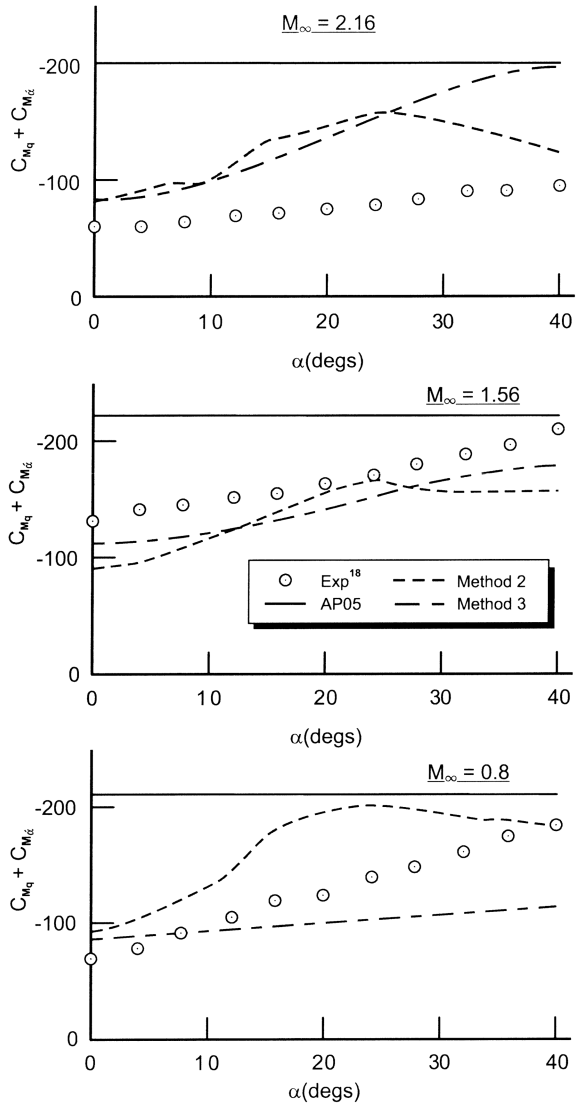

Fig. 10 Comparison of theory and experiment for pitch damping for MK82 low-drag bomb.

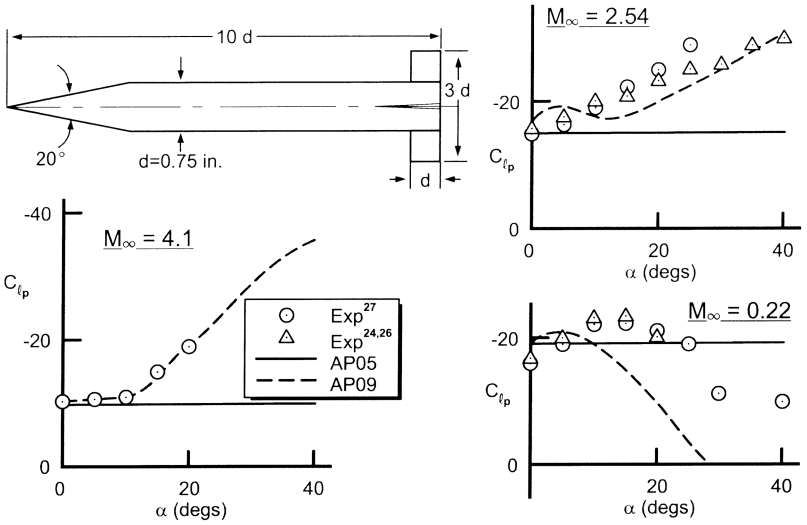

Fig. 11 Comparison of theory and experiment for roll damping of ANF.

configuration with comparisons to data at $M_\infty = 4.1$, 2.54, and 0.22 up to 90 deg in AOA.

Two sets of data are available for the $M_\infty = 0.22$ and 2.54 cases. One set of data is from AEDC [24,26] and the other data set from the former Naval Ordnance Laboratory (NOL) [27] (now part of AEDC). At $M_\infty = 4.1$, the new theory does an excellent job of following the data up to AOA 20 deg. At $M_\infty = 2.54$, the AP09 does a good job in following the trends of the data and is much more accurate than the AP05. At $M_\infty = 0.22$, the AP09 has the correct trend at both low and high AOA but overpredicts the loss of damping as AOA increases.

The second case considered is the modified finner where a more extensive database [24,26] exists. The configuration and results of comparison of the AP05 and AP09 theories to experiment are shown in Fig. 12. Results are shown for $M_\infty = 0.6$, 0.9, 1.3, 1.5, 2.0, 2.25, and 2.5 up to AOA 40 deg. In all cases, the AP09 gives the correct initial trend of the data and, at $M_\infty = 1.5$, 2.0, 2.25, and 2.5, compares very well to the data. At $M_\infty = 0.6$, the new theory compares well to experiment up to AOA 15 deg but does not predict the sharp dropoff in roll damping at $\alpha = 20$ deg. At $M_\infty = 0.9$, the AP09 overpredicts the maximum value of C_{ℓ_p} at AOA 10–15 deg but

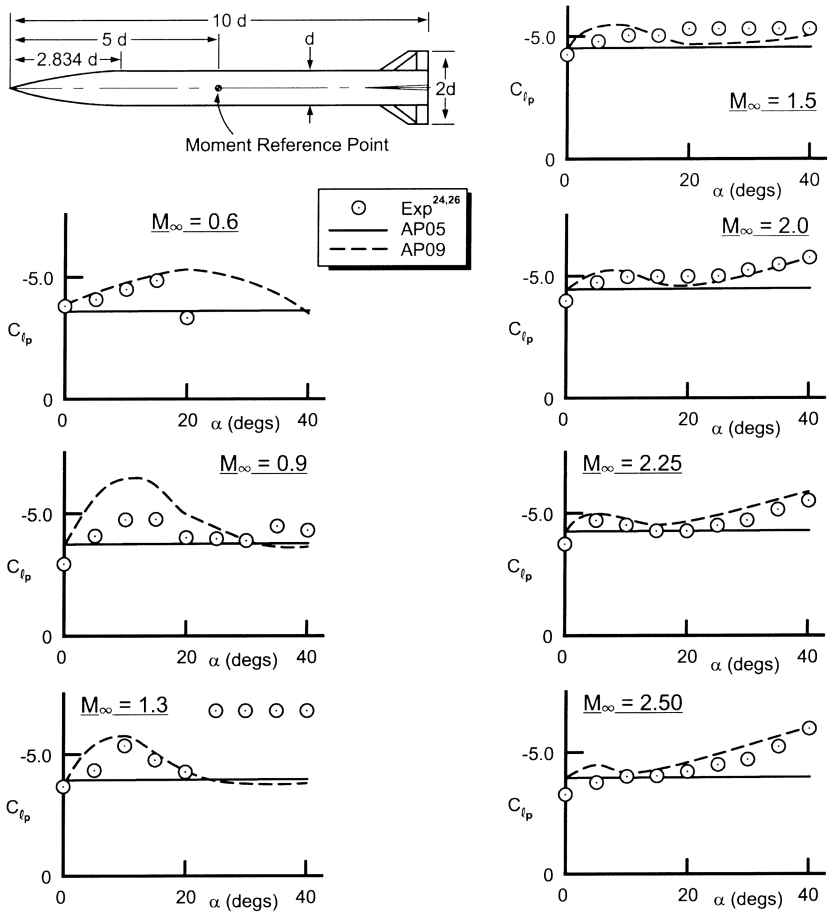

Fig. 12 Comparison of theory and experiment for roll damping of modified ANF.

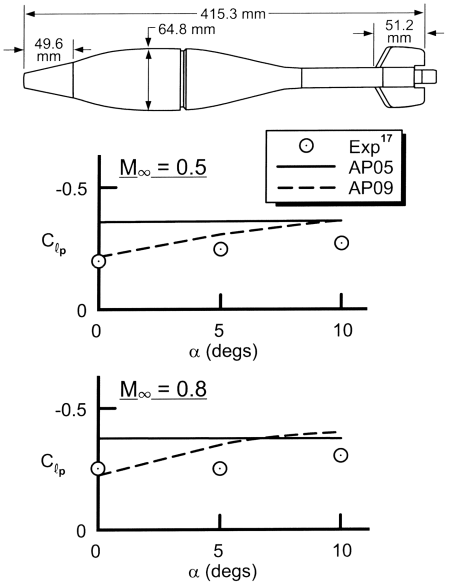

Fig. 13 Comparison of theory and experiment for roll damping of 81 mm mortar.

predicts the C_{ℓ_p} values at high AOA quite well. At $M_\infty = 1.3$, predictions are excellent up to $\alpha = 20$ deg where a sharp increase in C_{ℓ_p} data is noted at $\alpha = 25$ deg and higher. It is not clear what causes this sharp increase in C_{ℓ_p}, but wind-tunnel wall interference of the shock onto the tail is a possibility. In general, the AP09 nonlinear method is clearly superior to the linear AP05 roll damping methodology for the Fig. 12 configuration.

The next case considered is the 81 mm mortar configuration shown in Fig. 13. Comparison of theory and experiment up to 10 deg AOA at $M_\infty = 0.5$ and 0.8 is shown in the figure. The data suggest a slight nonlinearity in C_{ℓ_p} with increasing AOA, but not as large as predicted by the AP09. Even so, the AP09 roll damping predictions are still superior to those of the AP05.

The next two cases illustrate the capability of the AP09 to predict roll damping of configurations that have two sets of lifting surfaces. The first case is a canard controlled missile configuration shown in Fig. 14. Wind-tunnel tests [28,29] were conducted in a component buildup fashion which allows comparison of the AP05 and AP09 to body–canard, body–tail, and canard–body–tail configurations. Results are shown in Fig. 14 at $M_\infty = 0.1$ for AOA to 30 deg. In general, the comparison of the AP09 predictions to experiment is quite encouraging for all three configurations and is also superior to the AP05. Note the different trend of the body–tail data and body–canard data. The body–tail has a slight uptrend with α due to a moderate aspect ratio (1.33), whereas the body–canard has a decreasing trend with α due to a large aspect ratio (3.53). The higher aspect ratio wings stall and therefore lose lift curve slope, causing the decrease in roll damping capability. It is noteworthy that the roll damping of the canard–body–tail is much lower than the addition of the canard–body and body–tail cases added together. This lower value of C_{ℓ_p} for the complete configuration is due to the loss of roll damping effectiveness of the tails from the canard shed vortices. Note the canard shed vortex effects are reduced considerably at $\alpha = 25$ deg because the canard shed vortices have mostly passed over the tails. On the other hand, at $\alpha = 30$ deg, another complexity apparently has affected the roll damping, the asymmetric shedding of vortices. Note the large difference in roll damping moment on the canard–body–tail case at $\alpha = 30$ deg between two different wind-tunnel tests of the same model. Also note the sudden increase in C_{ℓ_p} for the body–tail case at $\alpha = 30$ deg. The implication of this figure is that, for subsonic speeds, the new nonlinear methodology of the AP09 is questionable above AOA 25 deg where asymmetric vortex shedding plays a role in the nonlinear aerodynamics.

The second canard–body–tail case is shown in Fig. 15. The Fig. 15 configuration has large wings and is quite similar in shape to a Sea Sparrow missile. According to the AP09 C_{ℓ_p} predictions, the tail surface loses all roll damping effectiveness at AOA 0. This also agrees with the flight tests results [30] and clearly shows the AP09 predictions to be superior to the AP05.

Although not shown on Fig. 15, the loss of tail damping with the canard–body–tail configuration of Fig. 15 is based on three separate AP09 runs where the body–tail, canard–body, and canard–body–tail are all considered individually. The C_{ℓ_p} values of Fig. 15 are basically those of the canard–body configuration. The tail values of C_{ℓ_p} are quite small due to a large wing-to-tail area and close proximity of the wing to tail, thus giving strong wing shed vortices at low AOA at the tail. The strong wing shed vortices eliminate not only most of the normal force of the tails, but roll damping as well.

Summary of AP09 Methods

Table 1 shows the evolution of the APC from its inception in 1972 (AP72) to the latest version, the AP09. As seen in Table 1, the AP09

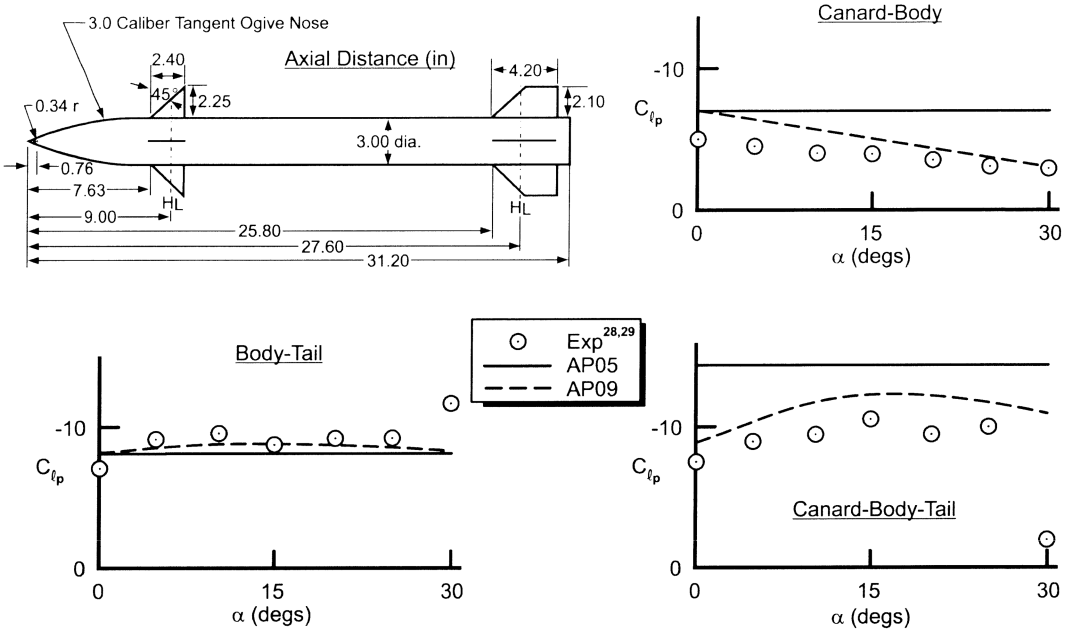

Fig. 14 Comparison of theory and experiment for roll damping for canard control missile configuration ($M_\infty = 0.1$).

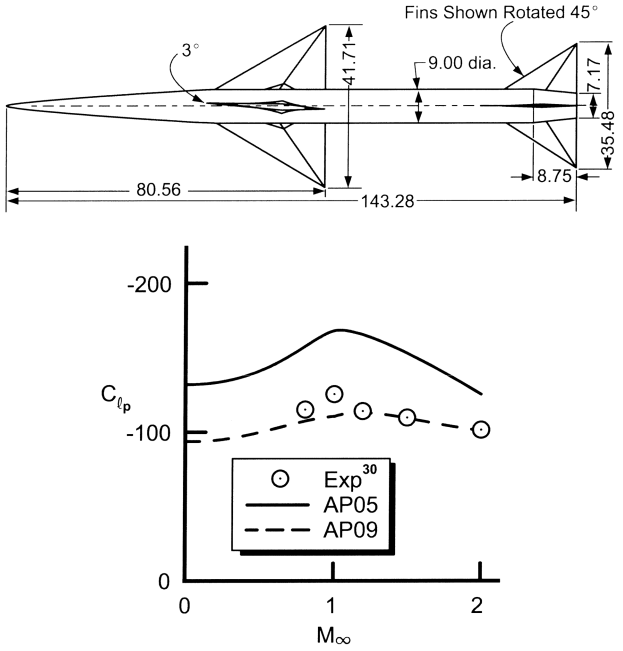

Fig. 15 Comparison of theory and flight tests for roll damping of wing–body–tail case at $\alpha \approx 0$.

now allows axisymmetric or nonaxisymmetric bodies, two sets of lifting surfaces, at flight conditions including Mach numbers up to 20 and AOA to 90 deg. The code can give trim aerodynamics, compute trajectories, compute convective heat transfer, and provide structural loads along with the basic nonlinear static and dynamic aerodynamics.

Tables 7–10 summarize the theoretical methods for the AP09. Methods in italics are the areas affected by the AP09. Table 7 gives the body-alone methods, Table 8 the wing and interference aerodynamic methods, Table 9 the dynamic derivative methods, and Table 10 the trajectory capability.

Conclusions

To summarize, significant new improvements and technology have been added to the next version of the Aeroprediction Code, the AP09. The major effect of the improvements is to improve the APC aerodynamic predictions for normal force, center of pressure, and roll and pitch damping for configurations that have boattails. Configurations include mortars, low-drag bombs, spin-stabilized projectiles, and missiles, in that order. In addition, new methods to predict nonlinear roll and pitch damping were developed and integrated into the Aeroprediction Code.

Comparison of the new methods to experimental data showed significant improvement of the AP09 over the AP05 in roll and pitch damping, center of pressure, and normal force prediction accuracy for configurations with boattails. Adding new nonlinear pitch and roll damping capability also significantly improved the AP09 prediction accuracy compared with experimental data for all weapon configurations.

The validation of the new nonlinear methodology for pitch and roll damping was hindered by the lack of generic databases that varied fin size, shape, location, and freestream conditions. For pitch damping wind-tunnel data, an additional concern of model to sting interference also existed. A truth model for roll and pitch damping, consisting of nonlinear experimental results backed up by full Navier–Stokes calculations, would greatly enhance refinement of the new nonlinear dynamic derivative semi-empirical models.

It is anticipated that the AP09 will be the last major upgrade of the APC. It is anticipated that new technology will continue to be developed and integrated into the code and given to those who have extended user support (EUS) in effect. Hence, those who have EUS will get an annual upgrade of the AP09 which will contain any corrections found as well as any new technology added. A new pricing structure is also anticipated for the AP09.

Table 7 AP09 methods for body-alone aerodynamics

Component/Mach number region	Subsonic $M_\infty < 0.8$	Transonic $0.8 \le M_\infty \le 1.2$	Low supersonic $1.2 \le M_\infty \le 1.8$	Mod/high supersonic $1.8 \le M_\infty \le 6.0$	Hypersonic $M_\infty > 6.0$
Nose wave drag	Improved empirical	Improved semi-empirical based on Euler solutions	Second-order Van Dyke plus MNT	Soset plus IMNT	Soset plus IMNT modified for real gases
Boattail or flare wave drag	——	Wu and Aoyoma	Second-order Van Dyke	Soset	Soset for real gases
Skin friction drag	Van Driest 2 with more boundary-layer transition options				
Base drag: power off	Improved empirical method: empirical				
power on	modified Brazzel method				
base bleed	modified Danberg method				
Axial force at α	*Empirical method*				
Aeroheating information	——		Soset plus IMNT for real gases		
Inviscid lift and pitching moment	*Empirical*	*Semi-empirical based on Euler solutions*	*Tsien first-order crossflow*	*Soset*	*Soset for real gases*
Viscous lift and pitching moment	Improved Allen and Perkins crossflow				
Nonaxisymmetric body aero lifting properties axial force	Modified Jorgensen Modified axisymmetric body				
Nonlinear st. loads avail., $\Phi = 0$, 45 deg	No		Yes		
Protuberance aero input options	Yes				
Accurate small caliber arms aero	Yes				

Table 8 AP09 methods for wing-alone and interference aerodynamics.

Component/Mach number region	Subsonic $M_\infty < 0.8$	Transonic $0.8 \le M_\infty \le 1.2$	Low supersonic $1.2 \le M_\infty \le 1.8$	Mod/high supersonic $1.8 \le M_\infty \le 6.0$	Hypersonic $M_\infty > 6.0$
Wave drag	Semi-empirical	Improved semi-empirical	Linear theory plus MNT	Shock expansion (SE) plus MNT along strips	SE plus MNT for real gases along strips
Skin friction drag	Van Driest 2 with more boundary-layer transition options				
Trailing-edge separation drag	Improved empirical				
Body base pressure caused by tail fins	Empirical				
Inviscid lift and pitching moment:	Lifting surface theory	Empirical	3DTWT	3DTWT	3DTWT
linear					
nonlinear					
impact of trailing edge–semi-empirical bluntness	Empirical				
Wing–body, body–wing interference, $\Phi = 0$, 45 deg	Slender body theory or linear theory modified for short afterbodies				
linear	Improved empirical				
nonlinear					
Wing–body interference due to δ, $\Phi = 0$, 45 deg	Slender body theory				
linear	Improved empirical				
nonlinear					
Wing–tail interference, $\Phi = 0$, 45 deg	Line vortex theory with modification for $K_{W(B)}$ term and nonlinearities				
Aeroheating	None present			SE plus MNT	SE plus MNT real gases
Nonaxisymmetric body aero, $\Phi = 0$, 45 deg	Improved Nelson method				
Nonlinear st. loads avail., $\Phi = 0$, 45 deg	No			Yes	
2, 3, 4, 6, 8 fin aero	Slender body theory				
linear	Semi-empirical, CFD + DATA				
nonlinear					
Trailing-edge flaps on tails	Semi-empirical (seek tail deflection for equal normal force)				

Table 9 AP09 methods for dynamic derivatives

Component/Mach number region	Subsonic $M_\infty < 0.8$	Transonic $0.8 \le M_\infty \le 1.2$	Low supersonic $1.2 \le M_\infty \le 1.8$	Mod/high supersonic $1.8 \le M_\infty \le 6.0$	Hypersonic $M_\infty > 6.0$
Body alone	*Empirical*				
no flare	*Semi-empirical*				
with flare	*Semi-empirical*				
nonlinear					
Wing and interference roll damping moment	*Lifting surface*		*Empirical*	*Linear thin wing theory*	
nonlinear	*Semi-empirical*		*Semi-empirical*	*Semi-empirical*	
Wing magnus moment	Assumed zero				
nonlinear					
Wing and interference pitch damping moment	*Lifting surface*		*Empirical*	*Linear thin wing theory*	
nonlinear	*Semi-empirical*		*Semi-empirical*	*Semi-empirical*	

Table 10 Trajectory and trim aerodynamics capability within APC

Simulation mode	AP72–AP98	AP02	AP05, AP09
Particle ballistic	None	Yes	Yes
3 degrees of freedom	None	Yes	Yes
Trim aero outputs	None	None	None

References

[1] Moore, F. G., "*Approximate Methods for Weapon Aerodynamics*," Vol. 186, Progress in Astronautics and Aeronautics, AIAA, Reston, VA, Aug. 2000.

[2] Moore, F. G., and Hymer, T. C., "The 2002 Version of the Aeroprediction Code, Part 1: Summary of New Theoretical Methodology," Naval Surface Warfare Center Dahgren Div., NSWCDD/TR-01-108, March 2002.

[3] Moore, F. G., and Hymer, T. C., "The 2005 Version of the Aeroprediction Code, Part 1: Summary of the New Methodology," Aeroprediction Rept. 1, Defense Technical Information Center, Alexandria, VA, Jan. 2004.

[4] Moore, F. G., and Moore, L. Y., "Improved Aerodynamics for Configurations with Boattails," *Atmospheric Flight Mechanics Conference*, AIAA Paper No. 6577, Aug. 2007.

[5] Moore, F. G., and Moore, L. Y., "New Methods to Predict Nonlinear Pitch Damping Moments," AIAA Paper No. 2008-0215, Jan. 2008.

[6] Moore, F. G., and Moore, L. Y., "A New Method to Predict Nonlinear Roll Damping Moments," *Fluid Dynamics Conference*, AIAA Paper No. 4375, June 2008.

[7] Moore, F. G., and Moore, L. Y., "The 2009 Version of the Aeroprediction Code: The AP09," Aeroprediction Rept. No. 3, Defense Technical Information Center, Alexandria, VA, Jan. 2008.

[8] Silton, S. I., "Navier–Stokes Computations for a Spinning Projectile from Subsonic to Supersonic Speeds," Army Research Lab. TR-2850, Sept. 2002.

[9] MacAllister, L. C., and Krial, K. S., "Aerodynamic Properties and Stability Behavior of the 155 mm Howitzer Shell M107," Ballistic Research Lab. Rept. No. 2547, Oct. 1975.

[10] Chadwick, W. R., and Sylvester, J. F., "Dynamic Stability of the 5″/54 Rocket Assisted Projectile," U.S. Naval Weapons Lab. TR-No. 2059, Oct. 1966.

[11] Ohlmeyer, E. J., "Dynamic Stability of the Improved 5″/54 Projectile," U.S. Naval Weapons Lab. TR-2871, Dec. 1974.

[12] Pierens, D., "Aerodynamic Evaluation of Production Fuzes and Fins for the 81 MM Improved Mortar Projectile," Defense Science Technology Office TR-0142, AR-008-331, March 1995.

[13] Malejke, G., "Static Aerodynamics for the 120 MM XM984 Extended

Range DPICM Mortar Projectile at Subsonic Mach Numbers," U. S. Army Armament Research Development and Engineering Center, TR ARAACCD-TR-00003, Jan. 2001.

[14] Owens, S., Dohren, R., and Malejke, G., "Test 101 (EMHSWT 1419), High Speed Wind Tunnel Test, Precision Guided Mortar Munition (PGMM)," Alliant Tech Systems, Test Rept., ATK Missile Systems Co., Rocket Center, WV, April 2005.

[15] Owens, S., Dohren, R., Sitts, J., and Malejko, G., "Test Report (Test 101B, Part 2) for the Precision Guided Mortar Munition (PGMM)," ATK Missile Systems Co. Contractor Rept. prepared for U.S. Army Research, Development, and Engineering Center, Picatinny Arsenal, NJ, 2002.

[16] Malejko, G., "Effect of Fuze Windshield Separation on Flight Performance of the 60-MM, HE, M494A Projectile with Fuze, RD, M935," U. S. Army Armament Research, Development and Engineering Center, TR ARAED-TR-93009, Aug. 1993; also Defense Technical Information Center, ADB175739.

[17] Pierens, D. A., "Pitch and Roll Damping Coefficients of the Australian 81 mm Improved Mortar Projectile," Defense Science Technology Office TR-0020, May 1994.

[18] Piper, W. D., and DeMeritte, F. J., "Summary of the NOL Investigations to Date of the Aerodynamic Characteristics of the Navy Low Drag Bomb," U.S. Naval Ordnance Lab. Rept. 5679, Feb. 1960.

[19] Anderson, C. F., and Carlton, W. E., "Static and Dynamic Stability Characteristics of the Fixed-Fin and Inflatable Stabilizer Retarder Configurations of the MK-82 Store at Transonic Speeds," Arnold Engineering Development Center TR 75-149 and Air Force Armament Test Lab. TR-75-141, Nov. 1975.

[20] Miklos, W. J., and Ingram, C. W., "Wind Tunnel Tests of Three Candidate MK 82 Snakeye Bomb Replacement Configurations," U.S. Air Force Research Lab. ARL-75-0174, June 1975; National Technical Information Service, U.S. Dept. of Commerce AD-A014-735, .

[21] Falkowski, E. W., "Transonic Aerodynamic Characteristics of a Full-Scale M117 Bomb with Three Fin Configurations," U.S. Army Munitions Command, TR 3785, Oct. 1968; Defense Technical Information Center AD 841577.

[22] Falkowski, E. W., "Subsonic Aerodynamic Characteristics of a 18 Percent Scale Model of the M117 750-lb Bomb with Folding Fins," Picatinny Arsenal, TR 4096, Dec. 1970; Defense Technical Information Center AD 878305.

[23] Uselton, B. L., and Uselton, J. C., "Test Mechanism for Measuring Pitch Damping Derivatives of Missile Configurations at High Angles of Attack," Arnold Engineering Development Center TR-75-43, May 1975; National Technical Information Service AD-A009-865.

[24] Uselton, B. L., and Jenke, L. M., "Experimental Missile Pitch and Roll Damping Characteristics at Large Angles of Attack," *Journal of Spacecraft and Rockets*, Vol. 14, No. 4, April 1977, pp. 241–247.

[25] Gillis, C. L., and Chapman, R., Jr., "Summary of Pitch-Damping Derivatives of Complete Airplane and Missile Configurations as Measured in Flight at Transonic and Supersonic Speeds," NACA RM L52K20, Jan. 1963.

[26] Jenke, L., "Experimental Roll-Damping, Magnus, and Static Stability Characteristics of Two Slender Missile Configurations at High Angles of Attack 0 to 90 Deg and Mach Numbers 0.2 through 2.5," Arnold Engineering Development Center TR-76-58, July 1976; Defense Technical Information Center AD A027027.

[27] Regan, F. J., "Roll Damping Measurements for the Basic Finner at Subsonic and Supersonic Speeds," U.S. Naval Ordnance Lab. Rept. 6652, March 1964.

[28] Hardy, S. R., "Nonlinear Rolling Motion Analysis of a Canard Controlled Missile Configuration at Angles of Attack from 0 to 30° in Incompressible Flow," Naval Surface Warfare Center Dahgren Div. TR-3808, May 1978.

[29] Hardy, S. R., "Subsonic Wind Tunnel Tests of a Canard-Control Missile in Pure Rolling Motion," Naval Surface Warfare Center Dahgren Div. TR-3615, June 1977.

[30] Hopko, R. N., "A Flight Investigation of the Damping in Roll and Rolling Effectiveness Including Aeroelastic Effects of Rocket-Propelled Missiles Having Cruciform, Triangular, Interdigitated Wings and Tails," NACA RM L51D16, Sept. 1951.

J. Martin
Associate Editor